We examined the expression of Fas and FasL at the small intestine by immunohistochemical analysis and found that indomethacin administration increased the expression of FasL, and this increase was suppressed in transgenic mice expressing HSP70 (Supplemental Fig. S5), suggesting that Fas/FasL interaction is involved in NSAID-induced apoptosis and its suppression by expression of HSP70 at the small intestine. It is also possible that high levels of proinflammatory cytokine secretion, which are reduced significantly by Hsp70, are responsible for suppression of NSAID-induced apoptosis by expression of HSP70 at the small intestine.

In addition to the cytoprotective effect of HSP70, an anti-inflammatory effect of HSP70 has also been reported. For example, up-regulation of HSP70 expression by heat shock inhibits the inflammatory stimuli-dependent activation of nuclear factor κB, which is responsible for inducing the production of various proinflammatory cytokines (Krappmann et al., 2004). We recently reported that the LPS-induced production of proinflammatory cytokines, including interleukin 1β and interleukin 6, was inhibited in peritoneal macrophages prepared from transgenic mice expressing HSP70 compared with their wild-type controls (Tanaka et al., 2007). As described above, inflammation plays an important role in the production of NSAID-induced lesions of the small intestine, and we found that the indomethacin-dependent elevation of intestinal MPO activity, an indicator of inflammation, was suppressed in transgenic mice expressing HSP70. Furthermore, we found that the indomethacin-induced expression of mRNA for some cytokines and chemokines (*il-1β*, *il-6*, and *mip-2*) in the small intestine was suppressed in transgenic mice expressing HSP70. We consider that expression of HSP70 suppresses the expression of these genes in the small intestine through its inhibitory effect on nuclear factor κB and that this effect is involved in the protective role of HSP70 against NSAID-induced lesions of the small intestine.

GGA has attracted considerable attention as an HSP inducer, largely because of its clinical value as an antiulcer drug and because it can induce HSPs without affecting cell viability (Hirakawa et al., 1996). We reported previously that GGA made cultured gastric cells resistant to indomethacin simultaneously with the up-regulation of expression of HSP70 (Tomisato et al., 2000). It was also reported that GGA made cultured intestinal cells resistant to oxidative stress simultaneously with the up-regulation of expression of HSP70 (Ohkawara et al., 2006). Furthermore, we found that preadministration of GGA not only increases the intestinal expression of HSP70 but also suppresses the production of indomethacin-induced lesions of the small intestine. The protection by GGA of the small intestine against NSAID-induced lesions was also reported recently (Kamei et al., 2008). These results strongly suggest that oral administration of GGA could also be therapeutically beneficial against NSAID-induced lesions of the small intestine in humans because of its HSP-inducing activity. However, because GGA mediates various other protective mechanisms, such as an increase in mucosal blood flow, stimulation of surface mucus production, and direct protection of cell membranes, these actions of GGA may also be involved in GGA-dependent protection against NSAID-induced lesions of the small intestine.

Gastroprotective drugs, such as GGA, have been used in the treatment of gastric lesions for a long period. However, it is believed that newly developed acid-control drugs (such as histamine-2 receptor antagonists and proton pump inhibitors) are superior to these gastroprotective drugs in curing and preventing gastric lesions. On the other hand, these acid-control drugs seem to be ineffective against NSAID-induced lesions of the small intestine, and the development of new molecules as candidate drugs to treat this disease must pass through the clinical trials process and may encounter the anticipated side effects. Thus, based on the results of this study, we propose that clinical studies be performed to prove the effectiveness of GGA for treating NSAID-induced lesions of the small intestine, given that the safety of GGA has already been shown clinically.

Acknowledgments

We thank Drs. C. E. Angelidis and G. N. Pagoulatos (University of Ioannina, Ioannina, Greece) for generously providing the mice.

References

Aabakken L, Bjørnbeth BA, Weberg R, Viksmoen L, Larsen S, and Osnes M (1990) NSAID-associated gastroduodenal damage: does famotidine protection extend into the mid- and distal duodenum? *Aliment Pharmacol Ther* **4**:295–303.

Adachi H, Katsuno M, Minamiyama M, Sang C, Pagoulatos G, Angelidis C, Kusakabe M, Yoshiki A, Kobayashi Y, Doyu M, et al. (2003) Heat shock protein 70 chaperone overexpression ameliorates phenotypes of the spinal and bulbar muscular atrophy transgenic mouse model by reducing nuclear-localized mutant androgen receptor protein. *J Neurosci* **23**:2203–2211.

Arai Y, Tanaka K, Ushijima H, Tomisato W, Tsutsumi S, Aburaya M, Hoshino T, Yokomizo K, Suzuki K, Katsu T, et al. (2005) Low direct cytotoxicity of nabumetone on gastric mucosal cells. *Dig Dis Sci* **50**:1641–1646.

Basivireddy J, Vasudevan A, Jacob M, and Balasubramanian KA (2002) Indomethacin-induced mitochondrial dysfunction and oxidative stress in villus enterocytes. *Biochem Pharmacol* **64**:339–349.

Boushey RP, Yusta B, and Drucker DJ (1999) Glucagon-like peptide 2 decreases mortality and reduces the severity of indomethacin-induced murine enteritis. *Am J Physiol Endocrinol Metab* **277**:E937–E947.

Goldstein JL, Eisen GM, Lewis B, Gralnek IM, Aisenberg J, Bhadra P, and Berger MF (2007) Small bowel mucosal injury is reduced in healthy subjects treated with celecoxib compared with ibuprofen plus omeprazole, as assessed by video capsule endoscopy. *Aliment Pharmacol Ther* **25**:1211–1222.

Gotoh T, Terada K, Oyadomari S, and Mori M (2004) hsp70-DnaJ chaperone pair prevents nitric oxide- and CHOP-induced apoptosis by inhibiting translocation of Bax to mitochondria. *Cell Death Differ* **11**:390–402.

Graham DY, Opekun AR, Willingham FF, and Qureshi WA (2005) Visible small-intestinal mucosal injury in chronic NSAID users. *Clin Gastroenterol Hepatol* **3**:55–59.

Hirakawa T, Rokutan K, Nikawa T, and Kishi K (1996) Geranylgeranylacetone induces heat shock proteins in cultured guinea pig gastric mucosal cells and rat gastric mucosa. *Gastroenterology* **111**:345–357.

Ishihara T, Hoshino T, Namba T, Tanaka K, and Mizushima T (2007) Involvement of up-regulation of PUMA in non-steroidal anti-inflammatory drug-induced apoptosis. *Biochem Biophys Res Commun* **356**:711–717.

Jacob M, Foster R, Sigthorsson G, Simpson R, and Bjarnason I (2007) Role of bile in pathogenesis of indomethacin-induced enteropathy. *Arch Toxicol* **81**:291–298.

Kamei K, Kubo Y, Kato N, Hatazawa R, Amagase K, and Takeuchi K (2008) Prophylactic effect of irsogladine maleate against indomethacin-induced small intestinal lesions in rats. *Dig Dis Sci* **53**:2657–2666.

Konaka A, Kato S, Tanaka A, Kunikata T, Korolkiewicz R, and Takeuchi K (1999) Roles of enterobacteria, nitric oxide and neutrophil in pathogenesis of indomethacin-induced small intestinal lesions in rats. *Pharmacol Res* **40**:517–524.

Krappmann D, Wegener E, Sunami Y, Esen M, Thiel A, Mordmuller B, and Scheidereit C (2004) The IkappaB kinase complex and NF-kappaB act as master regulators of lipopolysaccharide-induced gene expression and control subordinate activation of AP-1. *Mol Cell Biol* **24**:6488–6500.

Kunikata T, Tanaka A, Miyazawa T, Kato S, and Takeuchi K (2002) 16,16-Dimethyl prostaglandin E2 inhibits indomethacin-induced small intestinal lesions through EP3 and EP4 receptors. *Dig Dis Sci* **47**:894–904.

Lanas A and Ferrandez A (2006) NSAID-induced gastrointestinal damage: current clinical management and recommendations for prevention. *Chin J Dig Dis* **7**:127–133.

Maiden L, Thjodleifsson B, Seigal A, Bjarnason II, Scott D, Birgisson S, and Bjarnason I (2007) Long-term effects of nonsteroidal anti-inflammatory drugs and cyclooxygenase-2 selective agents on the small bowel: a cross-sectional capsule enteroscopy study. *Clin Gastroenterol Hepatol* **5**:1040–1045.

Maity P, Bindu S, Choubey V, Alam A, Mitra K, Goyal M, Dey S, Guha M, Pal C, and Bandyopadhyay U (2008) Lansoprazole protects and heals gastric mucosa from non-steroidal anti-inflammatory drug (NSAID)-induced gastropathy by inhibiting mitochondrial as well as Fas-mediated death pathways with concurrent induction of mucosal cell renewal. *J Biol Chem* **283**:14391–14401.

Mathew A and Morimoto RI (1998) Role of the heat-shock response in the life and death of proteins. *Ann N Y Acad Sci* **851**:99–111.

Matsumori Y, Hong SM, Aoyama K, Fan Y, Kayama T, Sheldon RA, Vexler ZS, Ferriero DM, Weinstein PR, and Liu J (2005) Hsp70 overexpression sequesters

AIF and reduces neonatal hypoxic/ischemic brain injury. *J Cereb Blood Flow Metab* **25**:899–910.

Morris AJ, Madhok R, Sturrock RD, Capell HA, and MacKenzie JF (1991) Enteroscopic diagnosis of small bowel ulceration in patients receiving non-steroidal anti-inflammatory drugs. *Lancet* **337**:520.

Morris AJ, Murray L, Sturrock RD, Madhok R, Capell HA, and Mackenzie JF (1994) Short report: the effect of misoprostol on the anaemia of NSAID enteropathy. *Aliment Pharmacol Ther* **8**:343–346.

Ohkawara T, Takeda H, Nishiwaki M, Nishihira J, and Asaka M (2006) Protective effects of heat shock protein 70 induced by geranylgeranylacetone on oxidative injury in rat intestinal epithelial cells. *Scand J Gastroenterol* **41**:312–317.

Reuter BK, Davies NM, and Wallace JL (1997) Nonsteroidal anti-inflammatory drug enteropathy in rats: role of permeability, bacteria, and enterohepatic circulation. *Gastroenterology* **112**:109–117.

Sigthorsson G, Simpson RJ, Walley M, Anthony A, Foster R, Hotz-Behoftsitz C, Palizban A, Pombo J, Watts J, Morham SG, et al. (2002) COX-1 and 2, intestinal integrity, and pathogenesis of nonsteroidal anti-inflammatory drug enteropathy in mice. *Gastroenterology* **122**:1913–1923.

Somasundaram S, Sigthorsson G, Simpson RJ, Watts J, Jacob M, Tavares IA, Rafi S, Roseth A, Foster R, Price AB, et al. (2000) Uncoupling of intestinal mitochondrial oxidative phosphorylation and inhibition of cyclooxygenase are required for the development of NSAID-enteropathy in the rat. *Aliment Pharmacol Ther* **14**:639–650.

Stankiewicz AR, Lachapelle G, Foo CP, Radicioni SM, and Mosser DD (2005) Hsp70 inhibits heat-induced apoptosis upstream of mitochondria by preventing Bax translocation. *J Biol Chem* **280**:38729–38739.

Suemasu S, Tanaka K, Namba T, Ishihara T, Katsu T, Fujimoto M, Adachi H, Sobue G, Takeuchi K, Nakai A and Mizushima T (2009) A role for HSP70 in protecting against indomethacin-induced gastric lesions. *J Biol Chem* doi:10.1074/jbc.M109.006817.

Tanaka A, Hase S, Miyazawa T, Ohno R, and Takeuchi K (2002) Role of cyclooxygenase (COX)-1 and COX-2 inhibition in nonsteroidal anti-inflammatory drug-induced intestinal damage in rats: relation to various pathogenic events. *J Pharmacol Exp Ther* **303**:1248–1254.

Tanaka A, Matsumoto M, Hayashi Y, and Takeuchi K (2005a) Functional mechanism underlying cyclooxygenase-2 expression in rat small intestine following administration of indomethacin: relation to intestinal hypermotility. *J Gastroenterol Hepatol* **20**:38–45.

Tanaka K, Namba T, Arai Y, Fujimoto M, Adachi H, Sobue G, Takeuchi K, Nakai A, and Mizushima T (2007) Genetic evidence for a protective role for heat shock factor 1 and heat shock protein 70 against colitis. *J Biol Chem* **282**:23240–23252.

Tanaka K, Tomisato W, Hoshino T, Ishihara T, Namba T, Aburaya M, Katsu T, Suzuki K, Tsutsumi S, and Mizushima T (2005b) Involvement of intracellular Ca^{2+} levels in nonsteroidal anti-inflammatory drug-induced apoptosis. *J Biol Chem* **280**:31059–31067.

Tang D, Kang R, Xiao W, Wang H, Calderwood SK, and Xiao X (2007) The anti-inflammatory effects of heat shock protein 72 involve inhibition of high-mobility-group box 1 release and proinflammatory function in macrophages. *J Immunol* **179**:1236–1244.

Tomisato W, Takahashi N, Komoto C, Rokutan K, Tsuchiya T, and Mizushima T (2000) Geranylgeranylacetone protects cultured guinea pig gastric mucosal cells from indomethacin. *Dig Dis Sci* **45**:1674–1679.

Tomisato W, Tsutsumi S, Hoshino T, Hwang HJ, Mio M, Tsuchiya T, and Mizushima T (2004) Role of direct cytotoxic effects of NSAIDs in the induction of gastric lesions. *Biochem Pharmacol* **67**:575–585.

Tsutsumi S, Gotoh T, Tomisato W, Mima S, Hoshino T, Hwang HJ, Takenaka H, Tsuchiya T, Mori M, and Mizushima T (2004) Endoplasmic reticulum stress response is involved in nonsteroidal anti-inflammatory drug-induced apoptosis. *Cell Death Differ* **11**:1009–1016.

Urayama S, Musch MW, Retsky J, Madonna MB, Straus D, and Chang EB (1998) Dexamethasone protection of rat intestinal epithelial cells against oxidant injury is mediated by induction of heat shock protein 72. *J Clin Invest* **102**:1860–1865.

Wallace JL (1994) The 1994 Merck Frosst Award. Mechanisms of nonsteroidal anti-inflammatory drug (NSAID) induced gastrointestinal damage–potential for development of gastrointestinal tract safe NSAIDs. *Can J Physiol Pharmacol* **72**:1493–1498.

Watanabe T, Sugimori S, Kameda N, Machida H, Okazaki H, Tanigawa T, Watanabe K, Tominaga K, Fujiwara Y, Oshitani N, et al. (2008) Small bowel injury by low-dose enteric-coated aspirin and treatment with misoprostol: a pilot study. *Clin Gastroenterol Hepatol* **6**:1279–1282.

Whittle BJ, László F, Evans SM, and Moncada S (1995) Induction of nitric oxide synthase and microvascular injury in the rat jejunum provoked by indomethacin. *Br J Pharmacol* **116**:2286–2290.

Address correspondence to: Dr. Tohru Mizushima, Graduate School of Medical and Pharmaceutical Sciences, Kumamoto University, 5-1 Oe-honmachi, Kumamoto 862-0973, Japan. E-mail: mizu@gpo.kumamoto-u.ac.jp

Pharmaceutical Research, Vol. 26, No. 10, October 2009 (© 2009)
DOI: 10.1007/s11095-009-9943-x

Research Paper

Accelerated Blood Clearance Phenomenon Upon Repeated Injection of PEG-modified PLA-nanoparticles

Tsutomu Ishihara,[1,2] Miho Takeda,[1] Haruka Sakamoto,[1] Ayumi Kimoto,[1] Chisa Kobayashi,[1] Naoko Takasaki,[1] Kanae Yuki,[1] Ken-ichiro Tanaka,[1] Mitsuko Takenaga,[3] Rie Igarashi,[3] Taishi Maeda,[1] Naoki Yamakawa,[1] Yoshinari Okamoto,[1] Masami Otsuka,[1] Tatsuhiro Ishida,[4] Hiroshi Kiwada,[4] Yutaka Mizushima,[2] and Tohru Mizushima[1,5]

Received May 24, 2009; accepted July 13, 2009; published online July 25, 2009

Purpose. We recently developed prostaglandin E_1 (PGE_1)-encapsulated nanoparticles, prepared with a poly(lactide) homopolymer (PLA, Mw=17,500) and monomethoxy poly(ethyleneglycol)-PLA block copolymer (PEG-PLA) (NP-L20). In this study, we tested whether the accelerated blood clearance (ABC) phenomenon is observed with NP-L20 and other PEG-modified PLA-nanoparticles in rats.
Methods. The plasma levels of PGE_1 and anti-PEG IgM antibody were determined by EIA and ELISA, respectively.
Results. Second injections of NP-L20 were cleared much more rapidly from the circulation than first injections, showing that the ABC phenomenon was induced. This ABC phenomenon, and the accompanying induction of anti-PEG IgM antibody production, was optimal at a time interval of 7 days between the first and second injections. Compared to NP-L20, NP-L33s that were prepared with PLA (Mw=28,100) and have a smaller particle size induced production of anti-PEG IgM antibody to a lesser extent. NP-L20 but not NP-L33s gave rise to the ABC phenomenon with a time interval of 14 days. NP-L33s showed a better sustained-release profile of PGE_1 than NP-L20.
Conclusions. This study revealed that the ABC phenomenon is induced by PEG-modified PLA-nanoparticles. We consider that NP-L33s may be useful clinically for the sustained-release and targeted delivery of PGE_1.

KEY WORDS: ABC phenomenon; anti-PEG IgM antibody; biodegradable nanoparticles; encapsulation; prostaglandin E_1.

INTRODUCTION

Nanoparticles such as liposomes, lipid emulsions and polymeric solid particles that are approximately 100–200 nm in diameter have been widely used as carrier systems for targeted drug delivery to tumors, inflammatory tissues and vascular lesions due to their enhanced permeability and retention (EPR) effects (1). However, this size of particles is easily captured by the mononuclear phagocyte system (MPS), or in other words by the reticuloendothelial system, resulting in rapid clearance from the circulation (2,3). Modification of the nanoparticle surface with poly(ethyleneglycol) (PEG) enables such nanoparticles to escape this uptake due to the steric barrier by which the PEG chain prevents interaction of the nanoparticles with opsonins and the cells responsible for MPS, such as Kupffer cells (stealth effect) (2–4). For example, doxorubicin-containing PEG-modified (PEGylated) liposomes are used clinically because, due to EPR effects, this formulation gives more potent anti-tumor activity and less drug-related toxicity than doxorubicin itself (5).

However, a pharmacokinetic issue for PEGylated liposomes, the so-called accelerated blood clearance (ABC) phenomenon, was recently revealed (6,7). In this phenomenon, a second dose of PEGylated liposomes is rapidly cleared from the circulation when administered within a certain time interval from the first dose injection due to their accelerated accumulation in the liver. This has been observed for a number of different animal species (8). The ABC phenomenon is of clinical concern because it decreases the

[1] Graduate School of Medical and Pharmaceutical Sciences, Kumamoto University, 5-1 Oe-honmachi, Kumamoto 862-0973, Japan.
[2] DDS Institute, The Jikei University School of Medicine, Tokyo 105-8461, Japan.
[3] Division of Drug Delivery System, Institute of Medical Science, St. Marianna University, Kawasaki 216-8512, Japan.
[4] Institute of Health Bioscience, The University of Tokushima, Tokushima 770-8505, Japan.
[5] To whom correspondence should be addressed. (e-mail: mizu@gpo.kumamoto-u.ac.jp)

ABBREVIATIONS: ABC, Accelerated blood clearance; ADAM, 9-anthryldiazomethane; AUC, Area under the blood concentration-time curve; CL, Total body clearance; DEA, diethanolamine; EPR, Enhanced permeability and retention; FBS, Fetal bovine serum; ^{1}H-NMR, Proton nuclear magnetic resonance; HPLC, High-performance liquid chromatography; MPS, Mononuclear phagocyte system; MQW, Milli-Q water; Mw, Molecular weight; PBS, Phosphate-buffered saline; PEG, Poly(ethyleneglycol); PGE1, Prostaglandin E1; PLA, Poly(lactide); QOL, Quality of life; S.E.M., Standard error mean.

0724-8741/09/1000-2270/0 © 2009 Springer Science + Business Media, LLC

121

therapeutic efficacy of an encapsulated drug upon repeated administration and may cause adverse effects due to altered biodistribution of the drug. The time interval between repeated injections, the dose and physicochemical properties of the PEGylated liposomes and species of encapsulated drugs were shown to affect the extent of the ABC phenomenon (8–14). Although the mechanism causing the ABC phenomenon is still unclear, it was recently proposed that this phenomenon involves sequential events, including induction of anti-PEG IgM antibody production in the spleen by the first dose of PEGylated liposomes, complement activation by the IgM antibody and opsonization by C3 fragments following the second dose of PEGylated liposomes, and their uptake by MPS (6,11,14–18).

The number of patients with peripheral obstructive vascular diseases, such as arteriosclerosis obliterans, has increased in line with aging of the population and increases in the prevalence of diabetes and hyperlipidemia (19). While various clinical treatments, such as vascular bypass surgery, have been developed for these diseases, the prognosis is still not good. Prostaglandin E_1 (PGE_1), which has various physiological actions, such as vasodilation, angiogenesis and inhibition of platelet aggregation, serves as an effective treatment for peripheral obstructive vascular diseases (20–22). However, when administered systemically, PGE_1 also has related adverse effects, such as hypotension and diarrhea (21,23). Furthermore, in addition to its chemical instability (hydrolysis to PGA_1), PGE_1 is easily inactivated by 15-hydroxydehydrogenase during its passage through the lung (24–26). In order to overcome these issues, we developed lipo-PGE_1, a preparation incorporating PGE_1 into an oil-in-water lipid emulsion consisting of a soybean oil core and lecithin surfactant with a diameter of approximately 200 nm (27–29). Incorporation of PGE_1 into lipid emulsion protects PGE_1 from inactivation in the lung and enables the selective delivery of PGE_1 to damaged blood vessels, resulting in enhanced therapeutic effects and reduced drug-related toxicity (27,30). However, lipid emulsion cannot retain PGE_1 for a long period *in vivo* (4,31). Therefore, daily intravenous drip infusion is necessary for clinical treatment with lipo-PGE_1, which in turn requires patient hospitalization, resulting in a low quality of life (QOL).

We recently developed another formulation of PGE_1 in which the PGE_1 is encapsulated in biodegradable and biocompatible polymeric solid particles prepared with poly(lactide) homopolymer (PLA) and monomethoxy poly(ethyleneglycol)-PLA block copolymer (PEG-PLA). These particles have a mean diameter of 120 nm, which enhances the selective delivery of PGE_1 to damaged blood vessels due to the EPR effect (4). We also achieved a good sustained-release profile of PGE_1 from the nanoparticles, which may permit a longer-lasting therapeutic effect (4). The use of PEG-PLA enabled the nanoparticles to escape uptake by MPS (4). Based on these data, we proposed that PGE_1-encapsulated PEG-modified PLA-nanoparticles are of significant clinical benefit, because a single administration of this formulation may maintain a certain level of PGE_1 around damaged blood vessels for 1–2 weeks; in other words, repeated administration of this formulation with a time interval of 1–2 weeks to patients with peripheral obstructive vascular diseases may improve the symptom without patient hospitalization (4). However, prior to applying this formulation for clinical use, it was necessary to test whether the ABC phenomenon is induced by these nanoparticles. In this study, we have found that the ABC phenomenon and the accompanying production of anti-PEG IgM antibody are induced by the intravenous administration of PGE_1-encapsulated PEG-modified PLA-nanoparticles. We successfully developed a modified formulation of the nanoparticles, which induces the ABC phenomenon *in vivo* to a lesser extent and shows a better sustained-release profile of PGE_1 *in vitro* than the original PGE_1-encapsulated PEG-modified PLA-nanoparticles.

MATERIALS AND METHODS

Materials and Animals

L-PLA (Mw=20,000 or 33,000 on the catalogue) was from Taki Chemical Co. Ltd. (Kakogawa, Japan). The molecular weights of the polymers were determined by gel permeation chromatography and were slightly different from the molecular weights specified in the catalogue. The molecular weight of L-PLA (Mw=20,000 or 33,000 on the catalogue) was determined to be 17,500 or 28,100, respectively. PEG-D,L-PLA (average molecular weight of PEG and PLA are 5,600 and 9,400, respectively) was synthesized and evaluated as described previously (4). PGE_1 was purchased from Cayman Chemical Co. (Osaka, Japan). Iron chloride and 1,4-dioxane were purchased from Wako Pure Chemicals Industries Ltd. (Osaka, Japan). 9-anthryldiazomethane (ADAM) was purchased from Funakoshi Co. Ltd. (Tokyo, Japan). Wistar rats (5–7 weeks old) were from Kyudo Co. Ltd. (Kumamoto, Japan). The rats were allowed free access to water and rat chow, and were housed under controlled environmental conditions (constant temperature, humidity and a 12 h dark-light cycle). The experiments and procedures described here were carried out in accordance with the Guide for the Care and Use of Laboratory Animals as adopted and promulgated by the National Institutes of Health, and were approved by the Animal Care Committee of Kumamoto University.

Detection of PGE_1 by High-Performance Liquid Chromatography (HPLC)

A Waters Alliance system running Empower software (Milford, MA) was used for HPLC analysis. Samples were separated using a 4.6×100-mm TSKgel Super-ODS column (Tosoh Co., Tokyo, Japan).

Solvent A (acetonitrile) and solvent B (Milli-Q water (MQW)) were used at a flow rate of 0.3 ml/min. Samples were incubated with ADAM at 37°C for 8 h. After injection of the sample (0 min), the mobile phase was changed as follows: 65% solvent A (25 min), a linear gradient of 65–100% solvent A (10 min) and then 100% solvent A (10 min). Fluorescence of ADAM reagent (excitation: 365 nm, emission: 412 nm) was detected using a 2475 Multi λ Fluorescence Detector.

ADAM is a fluorescent labelling reagent for carboxylic acids. ADAM is chemically unstable, but 9-anthrylmethyl ester derivative formed from ADAM and carboxylic acid is relatively stable (32). The derivative is sufficiently separated on a reversed-phase column and can be detected as reported

previously (4). The detection limit of PGE_1 in this method is approximately 50 ng/ml.

Preparation and Characterization of Nanoparticles

Nanoparticles were prepared by using the oil-in-water solvent diffusion method as described previously (4,33). L-PLA in 1,4-dioxane was mixed with PGE_1, PEG-D,L-PLA, iron chloride and diethanolamine (DEA) in acetone (the total amount of block copolymers and homopolymer was fixed at 25 mg). The different sizes of nanoparticles were prepared by altering the volume of 1,4-dioxane and acetone, as described previously (34). Samples were incubated for 10 min at room temperature and added to 25 ml of Milli-Q water (MQW) that stirred at 1,000 rpm. After addition of 0.5 ml of 0.5 M EDTA (pH 7.0) and 12.5 μl (62.5 μl for NP-L33s) of 200 mg/ml Tween 80, nanoparticles were purified and concentrated by ultrafiltration (Centriprep YM-50, Millipore Co., Billerica, MA). We have named the nanoparticles based on the isomer and molecular weight of PLA (from the catalogue). NP-L20 means nanoparticles (NP) prepared with L-PLA (L) of molecular weight 20,000 (as specified in the catalogue). NP-L20s means NP-L20 with a smaller particle size.

For determination of nanoparticle PGE_1 content, nanoparticles were dissolved in 150 μl of 1,4-dioxane and mixed with 150 μl of acetonitrile containing 3-phenylpropionate and 1.7 ml of 0.05 M EDTA (pH 3.6). After a 20 min incubation at room temperature, the solution was applied to a C18 reverse phase cartridge column (SepPak C18 200 mg, Waters, Milford, MA). After washing with 6 ml of MQW, PGE_1 was eluted with 3 ml of acetonitrile. The PGE_1 content was determined using HPLC, as described above. For determination of nanoparticle weight, the nanoparticle suspension was mixed with 0.05 M EDTA (pH 7.0) and centrifuged at 50,000 g for 30 min. The pellet was suspended in MQW, freeze-dried and weighed. The drug content was defined as the ratio of PGE_1 weight to the total weight of nanoparticles.

The PEG content of the nanoparticles was assayed as described previously (35) with some modifications. NaOH solution (4 N) was added to the nanoparticle suspension to give a final concentration of 0.8 N and incubated at 50°C for 24 h and neutralized by the addition of HCl solution (1 N). The mixtures were diluted in phosphate buffer (0.1 M, pH 7.4) and, following the addition of iodine and potassium iodide, the absorbance was read at 520 nm.

Particle size and distribution were determined by the dynamic light scattering method (ZETASIZER Nano-ZS, Malvern Instruments Ltd., Worcestershire, UK).

Pharmacokinetics of PGE_1-Encapsulated PLA-nanoparticles

The blood concentration profile of PGE_1 was monitored as described previously (4) with some modifications. PGE_1-encapsulated nanoparticles suspended in PBS were intravenously administered to rats via the tail vein. We used more than three rats for each group, and rats were assigned to each group, with the restriction that the groups were equated for average weight.

At the indicated periods, blood was collected from the tail vein using heparin-treated capillary tubes (Microhematocrit capillary tubes, Thermo Fisher Scientific, Yokohama, Japan), and 50 μl of each blood sample was mixed with 400 μl of 1,4-dioxane and 50 μl of 10 mM EDTA (pH 7.0) to extract PGE_1 from the nanoparticles. The mixture was centrifuged at 13,400 g for 10 min. The supernatant (200 μl) was evaporated to dryness and dissolved in 500 μl of PGE_1 enzyme immunoassay (EIA) buffer (R&D Systems Inc., Mineapolis, MN). Samples were centrifuged at 13,400 g for 2 min and the supernatant diluted appropriately. The PGE_1 content was determined using a PGE_1 EIA kit (R&D Systems Inc.) according to the manufacturer's protocol. $AUC_{(0-24)}$ is the area under the blood concentration-time curve from 0 to 24 h post-injection. The $AUC_{(0-24)}$ and total body clearance (CL) were calculated using the trapezium method by use of Microsoft Excel.

Determination of Anti-PEG IgM Antibody in Plasma

Quantification of IgM antibody reactive to PEG-PLA in plasma was determined by ELISA. All incubations were carried out at room temperature. PEG-PLA (10 nmol) in 50 μl ethanol was added to 96-well plates (EIA/RIA plate, AGC Techno Glass Co. Ltd., Funabashi, Japan) and air dried completely for 1 h. Then, 200 μl of blocking buffer (50 mM Tris/HCl (pH 8.0), 0.14 M NaCl and 1% BSA) was added and incubated for 1 h, and the wells were washed three times with washing buffer (50 mM Tris/HCl (pH 8.0), 0.14 M NaCl and 0.05% Tween 20). Plasma obtained by centrifugation (15 min, 2,700 g) of collected blood samples was then diluted appropriately and added to the wells to incubate for 1 h. The wells were washed five times with the washing buffer, and 100 μl of horseradish peroxidase (HRP)-conjugated antibody (0.2 μg/ml, goat anti-rat IgM IgG-HRP conjugate, Bethyl Laboratories, Inc., Montgomery, TX) in blocking buffer containing 0.05% Tween 20 was added to each well. After incubation for 1 h, the wells were washed five times with washing buffer. Coloration was initiated by adding *o*-phenylene diamine (1 mg/ml) (Sigma, St. Louis, MO) and stopped by adding 100 μl of 2 M H_2SO_4 after a 5 min incubation. The absorbance was measured at 490 nm using a Microplate reader (FLUOstar, BMG LABTECH Ltd., Offenburg, Germany).

RESULTS

Induction of the ABC Phenomenon and Production of Anti-PEG IgM Antibody

In general, hydrophilic drugs such as PGE_1 are very hard to encapsulate in PLA-nanoparticles. We recently succeeded in encapsulating PGE_1 by precipitating PGE_1 with iron ions (4). In that previous report, we prepared various types of PLA-nanoparticles. Of them, NP-L20, which was prepared with L-PLA (Mw=17,500) and PEG-D,L-PLA and had a mean diameter of 120 nm, showed a good sustained-release profile of PGE_1 (the half life *in vitro* was about 10 days), a relatively good efficiency of encapsulation (about 1% drug content) and a long blood residence time (4). Thus, in the current study, we have tested whether NP-L20 induces the ABC phenomenon.

We estimated the clinical dose of PGE_1-encapsulated nanoparticles is 120 μg PGE_1 for individual human (about 2 μg PGE_1/kg) because lipo-PGE_1 at 5–10 μg PGE_1/day is

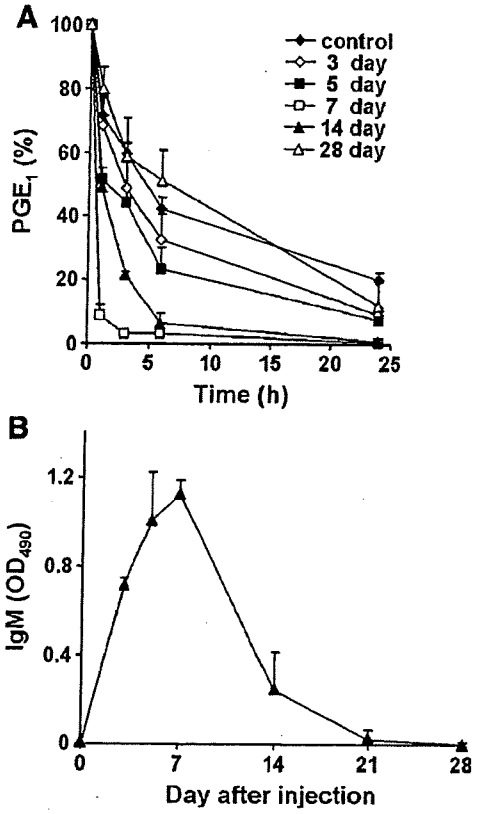

Fig. 1. Induction of the ABC phenomenon and production of anti-PEG IgM antibody by repeated administration of NP-L20. **A** Rats were intravenously administered NP-L20 (50 μg nanoparticles/rat). At 3, 5, 7, 14 or 28 days after the injection, NP-L20 (1,000 μg nanoparticles/rat) was intravenously administered. Plasma PGE_1 levels were monitored after injection of the second dose as described in the "Materials and Methods" and shown relative to the initial level. As a control, alteration of plasma PGE_1 levels following administration of NP-L20 (1,000 μg nanoparticles/rat) to naïve rats is shown. Values are given as mean ± S.E.M. (n=3–10) **B** Rats were intravenously administered NP-L20 (50 μg nanoparticles/rat) and blood samples were prepared periodically. The amount of anti-PEG IgM antibody was determined by ELISA as described in "Materials and Methods." Values are mean ± S.E.M. (n=3).

used clinically, and we assumed that the sustained-release formulation would be delivered as one injection per 2 weeks. Thus, we used a dose of 50 μg NP-L20 for individual rat (about 2 μg PGE_1/kg) for the first injection. We examined the pharmacokinetics of PLA-nanoparticles by determining the plasma level of PGE_1; a pilot study revealed that about 1,000 μg NP-L20 (about 10 μg PGE_1) was required for this detection (data not shown). Therefore, we used a dose of 1,000 μg NP-L20 for individual rat for the second injection. However, it is possible that the increased dosing results in higher uptake by liver and leads to clearance.

Rats were administered NP-L20 twice at a time interval of 3, 5, 7, 14 or 28 days, and the pharmacokinetic behaviour (blood clearance profile) of the second dose of NP-L20 was investigated by measuring plasma concentration of PGE_1, and the behaviour was compared to that without a prior injection (control). As shown in Fig. 1A, compared to the control, more rapid clearance of NP-L20 was observed after injection of the second dose, indicating that the ABC phenomenon was induced by the injection of the first dose. The ABC phenomenon was most apparent at the time interval of 7 days between the first and second injections, and the phenomenon was not so apparent at a time interval of 3 or 14 days, showing that the ABC phenomenon induced by PEG-modified PLA-nanoparticles is dependent on the time interval, as reported for PEGylated liposomes (14). A strong inverse relationship between the dose of initially injected PEGylated liposomes and the extent of the ABC phenomenon was reported (10,36). But we found that induction of the ABC phenomenon by NP-L20 was not so clearly affected by the initial dose (from 1 μg to 1 mg NP-L20; data not shown).

We also measured the plasma levels of IgM antibodies reactive to PEG-PLA after injection of 50 μg NP-L20 by use of a modified ELISA with PEG-PLA-coated 96-well plates. The production reached its maximum level at day 7 post-injection and returned to the original level until day 28 post-injection (Fig. 1B). This time course correlates with the time course for induction of the ABC phenomenon (Fig. 1A), suggesting that IgM antibodies reactive to PEG-PLA are responsible for the ABC phenomenon. However, the amount of anti-PEG IgM antibody did not completely correlate with the level of ABC phenomenon: the level of IgM antibody at day 3 after the injection of first dose was higher than that at day 14 after, whereas the level of the ABC phenomenon showed the opposite trend (Fig. 1).

When the ELISA was performed with PLA-coated wells, production of IgM antibodies was not observed, (data not shown). On the other hand, when the ELISA was performed with PEG-coated wells, production of IgM antibodies was observed; however, the level was less than that observed with PEG-PLA-coated plates (data not shown), suggesting that the

Table I. Characteristics of PGE_1-Encapsulated PLA-nanoparticles Containing Different Amounts of PEG

Codes	L-PLA Mw (kDa)	PEG content (%)	PGE_1 content (%)	Particle size (nm)
PEG 0	17.5	0	1.01±0.14	154±4
PEG 7	17.5	5.4±0.5	0.86±0.09	120±2
PEG11	17,5	9.8±0.9	0.60±0.03	110±3
PEG18	17.5	12.8±0.3	0.92±0.34	109±3
PEG30	17.5	23.7±1.2	1.11±0.10	119±2

Nanoparticles encapsulating PGE_1 were prepared with L-PLA (Mw=17 500)/PEG-D,L-PLA (25 mg/0 mg, 22 mg/3 mg, 21 mg/4 mg, 18 mg/7 mg and 13 mg/12 mg for preparation of PEG0, PEG7, PEG11, PEG18 and PEG30 (NP-L20), respectively) in the presence of 5 mg PGE_1, 1.2 mg iron chloride and 4.8 mg DEA by an oil-in-water solvent diffusion method. The amounts of PEG in prepared nanoparticles were determined and the PEG content (w/w) is shown. PGE_1 content and nanoparticle size were determined as described in "Materials and Methods." Values are mean ± S.E.M. (n=3).

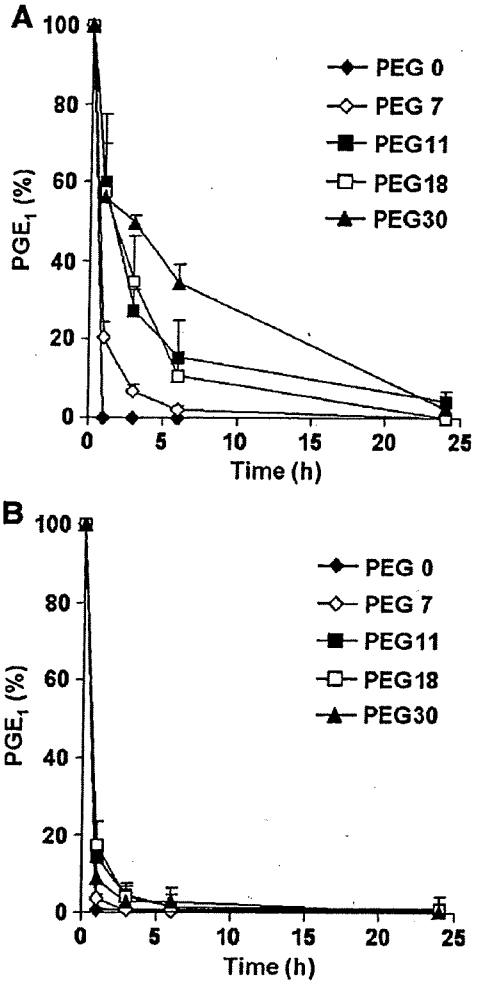

Fig. 2. The effect of PEG content of PLA-nanoparticles on their clearance from the circulation and on induction of the ABC phenomenon. **A** Various types of nanoparticles (PEG0, PEG7, PEG11, PEG18 and PEG30 (NP-L20)) were prepared as described in the legend of Tables I and II. Rats were intravenously administered PEG0, PEG7, PEG11, PEG18 or PEG30 (133 μg PGE_1/kg). Plasma PGE_1 levels were monitored and are shown as described in the legend of Fig. 1. Values are mean ± S.E.M. (n=3–4) **B** Rats were intravenously administered PEG0, PEG7, PEG11, PEG18 or PEG30 (50 μg nanoparticles/rat). After 7 days, the same type of nanoparticles (1,000 μg nanoparticles/rat) was administered and the amount of PGE_1 in plasma was monitored and shown as described above. Values are mean ± S.E.M. (n=3–6).

induced IgM antibodies recognize PEG rather than PLA, as reported for PEGylated liposomes (11).

Effect of the PEG Content of Nanoparticles on Induction of the ABC Phenomenon

It was reported that PEG content in PEGylated liposomes affects induction of the ABC phenomenon (36). Here we prepared PGE_1-encapsulated nanoparticles in the presence of various ratios of PLA and PEG-PLA (PEG30 means the nanoparticles prepared in the presence of 30% PEG (w/w); the real content of PEG in the prepared nanoparticles is shown in Table I). The particle size and the efficiency of encapsulation (PGE_1 content in nanoparticles) were similar for these types of nanoparticles (PEG0, PEG7, PEG11, PEG18 and PEG30), except that the particle size of PEG0 was larger than other types of nanoparticles (Table I).

We first examined the blood clearance profiles of the various types of nanoparticles following their intravenous injection into naïve rats in an attempt to understand their stealth effects. As shown in Fig. 2A, more rapid clearance from the circulation was observed with nanoparticles with lower PEG content, confirming that PEG confers the stealth effect of PLA-nanoparticles. Pharmacokinetic parameters ($AUC_{(0-24)}$ and CL) support this notion: approximately, $AUC_{(0-24)}$ became higher but CL became lower with the increase in the PEG content of nanoparticles (Table II). We then examined induction of the ABC phenomenon by these types of nanoparticles in a manner similar to the experiment summarized in Fig. 1A. Injection of a second dose of each of any of the types of nanoparticles at the time interval of 7 days resulted in very rapid clearance from the circulation (Fig. 2B). To evaluate the ABC phenomenon, we calculated the ratio of $AUC_{(0-24)}$ for the second injection (Fig. 2B) to that of the first one (Fig. 2A) as the ABC index; a value of 1 for this index means no induction of the ABC phenomenon. As shown in Table II, the ABC indexes for all types of nanoparticles except PEG0 were less than 1, and there is no apparent relationship between PEG content and the ABC index, showing that PEG-modified PLA-nanoparticles induce the ABC phenomenon irrespective of their PEG content. Based on the results in Fig. 2 and Table I, we fixed the PEG content at 30% because this achieved a good stealth effect, and we tried to find another way to suppress the ABC phenomenon.

Effect of Particle Size and Molecular Weight of PLA in Nanoparticles on Induction of the ABC Phenomenon

For PEGylated liposomes, it was reported that their size and physicochemical properties affect their ability to induce the ABC phenomenon (8). We have also reported that use of L-PLA of higher molecular weight improves the sustained-release profile of PGE_1 from nanoparticles (4). Thus, we prepared various types of nanoparticles with different diameters and compositions (NP-L20s, NP-L33 and NP-L33s). NP-L33 and NP-L33s were prepared from L-PLA (Mw=28,100), and NP-L20s and NP-L33s have a smaller particle size than NP-L20 and NP-L33 (Table III). The efficiency of encapsulation of PGE_1 was lower in nanoparticles with smaller size or

Table II. Characteristics of PGE_1-Encapsulated PLA-nanoparticles Containing Different Amounts of PEG

Codes	$AUC_{(0-24)}$ (μg·h/ml)	CL (ml/h·kg)	ABC index
PEG 0	0.39±0.13	401.0±97.7	1.43±0.14
PEG 7	0.93±0.07	143.9±10.5	0.53±0.02
PEG11	3.22±0.66	45.5±10.4	0.24±0.04
PEG18	2.98±0.51	47.9±9.8	0.41±0.08
PEG30	6.34±0.58	21.5±2.0	0.20±0.04

Pharmacokinetic parameters were calculated by moment analysis of the results shown in Fig. 2A. The ABC index was calculated as follows: ABC index = AUC of the second dose (Fig. 2B)/AUC of the first dose (Fig. 2A). Values are mean ± S.E.M. (n=4).

Table III. Characteristics of Various PGE_1-Encapsulated Nanoparticles with Different Diameters and Compositions

Codes	L-PLA Mw (kDa)	PEG content (%)	PGE_1 content (%)	Particle size (nm)
NP-L20	17.5	23.7±1.2	1.11±0.10	119±2
NP-L20s	17.5	28.7±1.8	0.86±0.04	81±6
NP-L33	28.1	30.4±0.8	0.83±0.17	134±4
NP-L33s	28.1	23.8±1.6	0.20±0.01	69±2

Nanoparticles encapsulating PGE_1 were prepared with 13 mg L-PLA (Mw=17 500) or L-PLA (Mw=28 100) and 12 mg PEG-D,L-PLA in the presence of 5 mg PGE_1, 1.2 mg iron chloride and 4.8 mg DEA by an oil-in-water solvent diffusion method. The nanoparticles were characterized as described in the legend of Tables I and II. Values are given as mean ± S.E.M. (n=3).

in those prepared from longer L-PLA (Table III). As a result, the PGE_1 content of NP-L33s was less than one-fifth of that of NP-L20 (Table III). At first, we compared the induction of anti-PEG IgM antibody after injection of these types of nanoparticles. As shown in Fig. 3A, compared to NP-L20, NP-L33s induced anti-PEG IgM antibody production to a lesser extent: the maximum level was lower and the level returned to the original level more rapidly. In addition, the induction of anti-PEG IgM antibody by NP-L20s or NP-L33 was less apparent than that by NP-L20; however, the difference was not as apparent as for NP-L33s (Fig. 3A).

We then examined induction of the ABC phenomenon by the various types of nanoparticles. As well as NP-L20, NP-L20s and NP-L33 gave rise to the ABC phenomenon when the second dose was injected at day 7 or 14 after injection of the first dose. However, they induced the phenomenon to a lesser extent than NP-L20 (Fig. 3B and Table IV). In contrast, NP-L33s did not exhibit the ABC phenomenon when the second dose was injected at day 14 after the first injection (Fig. 3B and Table IV). The ABC phenomenon was not apparent for any of the nanoparticles when the second dose was injected at day 28 after the injection of first dose (Fig. 3B and Table IV). The results for the ABC phenomenon shown in Fig. 3B correlate well with the induction of anti-PEG IgM antibody production shown in Fig. 3A, supporting the notion that anti-PEG IgM antibody is responsible for the ABC phenomenon. The results in Fig. 3B also show that NP-L33s has the better stealth effect than NP-L20 (Table IV).

Release Profile of PGE_1 from Nanoparticles *In Vitro*

Considering the clinical setting, the time interval of repeated injections of PGE_1-encapsulated nanoparticles could be prolonged with improvement of the sustained-release profile of PGE_1. Thus, we examined the release profile of PGE_1 from the NP-L20, NP-L20s, NP-L33 and NP-L33s upon incubation at 37°C in 50% fetal bovine serum (FBS) *in vitro* (Fig. 4). Since the concentration of PGE_1 in the medium (i.e. released PGE_1) was below the limits of detection in the preliminary experiment, the amount released was determined by measuring the PGE_1 remaining in the particles. We separated the nanoparticles from the medium by centrifugation (69,000 g for 30 min).

As shown in Fig. 4, NP-L20 showed a release profile similar to that observed in a previous paper (4) and more than half of the encapsulated PGE_1 was released from NP-L20 within 14 days. As suggested in previous reports (37,38), use of PLA with higher molecular weight resulted in a better sustained-release profile (Fig. 4). Furthermore, although the underlying mechanism is unknown, NP-L20s and NP-L33s showed better sustained-release profiles than NP-L20 and NP-L33, respectively (Fig. 4). This result is surprising, because it is generally believed that drug release from smaller size particles is faster due to the higher surface area. One possible explanation is that the distribution of PGE_1 in nanoparticles is not uniform and this distribution is affected by size of nanoparticles. Nevertheless, NP-L33s showed the best sustained-release profile, and more than half of the encapsulated PGE_1 remained in NP-L33s even after incubation for 28 days. These results suggest that NP-L33s is beneficial, not only because it results in less ABC phenomenon-inducing activity but also because it exhibits a better sustained-release profile of encapsulated PGE_1.

DISCUSSION

In order to develop a new formulation of PGE_1 that enables targeting and sustained-release drug delivery, we incorporated PGE_1 into PEG-modified PLA-nanoparticles (4). Before applying this formulation to a clinical setting, it is necessary to test whether it induces the ABC phenomenon, because this phenomenon may decrease the therapeutic efficacy of an encapsulated drug upon repeated administration. Consequently, in this study, we found that the ABC phenomenon is induced by the PEG-modified PLA-nanoparticles. Furthermore, we examined the mechanism underlying this phenomenon and could develop modified PGE_1-encapsulated nanoparticles that are less active in inducing the ABC phenomenon and show a better sustained release profile for encapsulated PGE_1.

The ABC phenomenon was identified for PEGylated liposomes, and its mechanism has been studied extensively for these liposomes (8). It was recently reported that the ABC phenomenon can also be induced by polymeric micelles (39,40). Here we have shown that the phenomenon can be induced by PEG-modified PLA nanoparticles, suggesting that the phenomenon is induced not specifically by PEGylated liposomes but generally by PEG-modified nanoparticles. Although it was reported that production of anti-PEG IgM antibody is induced by PEG-modified proteins in humans (41), it is not clear whether the ABC phenomenon is induced in humans. However, this possibility should be considered when PEG-modified nanoparticles are applied clinically in repeated intravenous administration.

Here we have examined which factors (time interval, dose, PEG content, molecular weight of PLA and particle size) affect induction of the ABC phenomenon by PEG-modified PLA-nanoparticles, referring to results for PEGy-

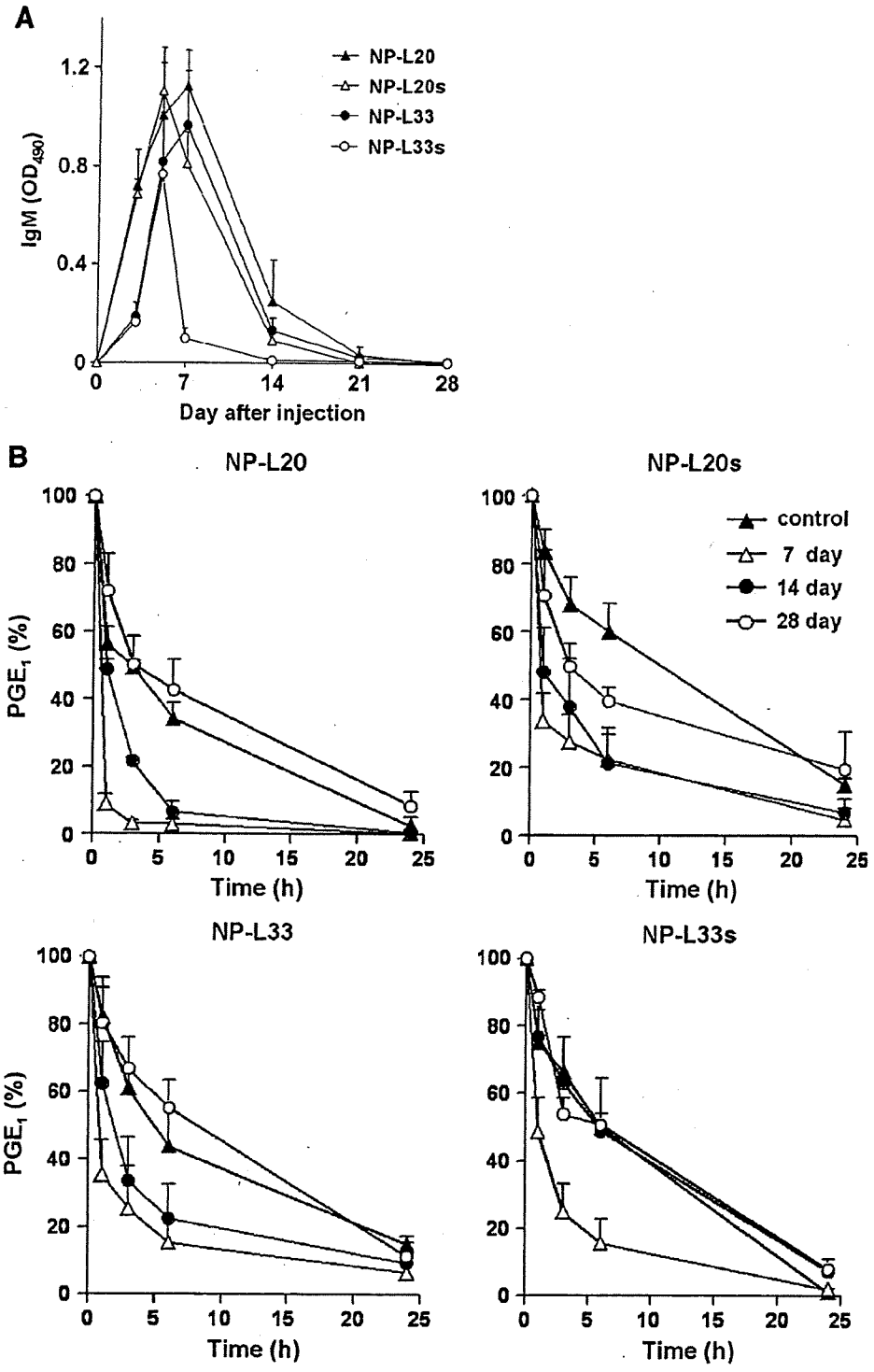

Fig. 3. Effect of molecular weight of L-PLA and particle size on induction of the ABC phenomenon and production of IgM antibody. **A** Various types of nanoparticles (NP-L20, NP-L20s, NP-L33 and NP-L33s) were prepared as described in the legend of Tables III and IV. Rats were intravenously administered each type of nanoparticle (50 μg nanoparticles/rat), and blood samples were taken periodically. The amount of anti-PEG IgM antibody was determined as described in the legend of Fig. 1. The NP-L20 data are the same as those in Fig. 1B. Values are mean ± S.E.M. (n=3–4). **B** Rats were intravenously administered each type of nanoparticle (50 μg nanoparticles/rat). At days 7, 14 or 28 days after the first injection, the same type of nanoparticles (1,000 μg nanoparticles/rat) was administered and the plasma PGE_1 levels were monitored and shown as described in the legend of Fig. 1. As a control, changes in plasma PGE_1 levels after the administration of each type of nanoparticles to naïve rats are shown. Values are mean ± S.E.M. (n=3–7).

Table IV. Characteristics of Various PGE_1-Encapsulated Nanoparticles with Different Diameters and Compositions

Codes	$AUC_{(0-24)}$ (μg·h/ml)	CL (ml/h·kg)	ABC index		
			7 day	14 day	28 day
NP-L20	6.35±0.58	21.5±2.0	0.17±0.03	0.39±0.04	1.26±0.25
NP-L20s	8.11±0.72	16.8±1.3	0.40±0.12	0.45±0.17	0.80±0.13
NP-L33	6.55±1.24	21.6±3.4	0.42±0.17	0.60±0.22	1.19±0.16
NP-L33s	7.59±0.76	18.0±1.8	0.43±0.12	1.06±0.19	1.07±0.05

Pharmacokinetic parameters were calculated based on the results shown in Fig. 3. The results were analysed as described in the legend of Tables I and II. Values are shown as mean ± S.E.M. (n=4).

lated liposomes. The time interval between injections clearly affected the ABC phenomenon: repeated injection of PEG-modified PLA-nanoparticles with a time interval of 7 days showed strongest induction of the phenomenon. Similar results were obtained for PEGylated liposomes (14). Doses (data not shown) or PEG content (Fig. 2) of the nanoparticles that were initially injected did not affect induction of the ABC phenomenon within the ranges of 1–1,000 μg PLA-nanoparticles (0.002–0.2 μmol PLA/kg) or 7–30% PEG content, respectively. Doses of the nanoparticles injected did not affect induction of the anti-PEG IgM antibodies within the ranges of 1–1,000 μg nanoparticles (data not shown). It was reported that a strong inverse relationship between the dose of initially injected PEGylated liposomes and the extent of the ABC phenomenon within the range of 0.001–5 μmol phospholipid/kg was observed and that PEG density beyond 5% suppressed induction of the ABC phenomenon (36). Thus, the effects of dose and PEG content of the initially injected nanoparticles on induction of the ABC phenomenon seem to differ depending on the types of nanoparticles. Smaller PEG-modified PLA-nanoparticles tended to induce the phenomenon to a lesser extent, which is in contrast to results observed for PEGylated liposomes (9). We also found that nanoparticles prepared from L-PLA (Mw=28,100) are less active for induction of the ABC phenomenon than those derived from L-PLA (Mw=17,500).

As for the mechanism for induction of the ABC phenomenon by PEG-modified PLA-nanoparticles, we suggest that anti-PEG IgM antibodies play an important role. The reason for this is that induction of anti-PEG IgM antibody by the first dose of nanoparticles and the magnitude of the ABC phenomenon observed after the second dose was generally well correlated. As pointed out for PEGylated liposomes (6,11,14–18), anti-PEG IgM antibodies induced by the first dose of PEG-modified PLA-nanoparticles may activate the complement system and opsonization by C3 fragments on the second dose, resulting in their uptake by MPS. However, the amount of anti-PEG IgM antibody did not completely correlate with the level of ABC phenomenon, as described above. Thus, a mechanism other than induction of production of anti-PEG IgM antibody may also be involved in this ABC phenomenon for PEG-modified PLA-nanoparticles.

Considering the potential clinical application of PGE_1-encapsulated PEG-modified PLA-nanoparticles, factors other than the ABC phenomenon (such as stealth effects and sustained-release profile) are also important. From this point of view, we propose that NP-L33s may be clinically beneficial as a targeted and sustained-release formulation of PGE_1 based on the following results from this study: (i) NP-L33s caused the weakest induction of production of anti-PEG IgM antibody and ABC phenomenon of the various types of nanoparticles, and no apparent ABC phenomenon was observed when these nanoparticles were repeatedly injected at an interval of 14 days; (ii) NP-L33s showed good stealth effect; (iii) NP-L33s showed the best sustained-release profile *in vitro*, and more than half of the encapsulated PGE_1 remained in the nanoparticles even after incubation for 28 days. Thus, if NP-L33s delivered to damaged blood vessels *in vivo* shows a similar sustained-release profile, it might keep the desired level of PGE_1 around the vessels upon repeated injection of once per 2 weeks or once per month without induction of the ABC phenomenon. However, since the optimum time interval for induction of the ABC phenomenon differs depending on the animal species for PEGylated liposomes (8,13), induction of the ABC phenomenon by NP-L33s in humans also needs to be examined.

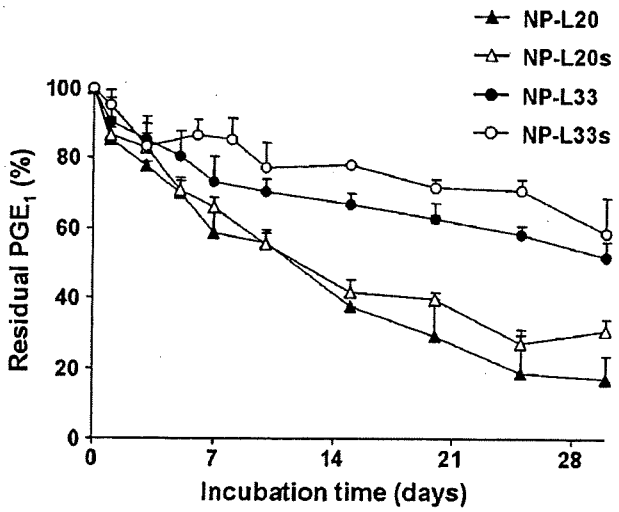

Fig. 4. Release profile of PGE_1 from nanoparticles *in vitro*. Various types of nanoparticles (NP-L20, NP-L20s, NP-L33 and NP-L33s) were prepared as described in the legend of Tables III and IV. Nanoparticles (at a particle concentration of 10 mg/ml) were dispersed in 50% FBS in PBS (*v/v*, 100 μl) and incubated at 37°C for the indicated periods. The PGE_1 content remaining in the nanoparticles as a function of time was determined by HPLC. Values shown are mean ± S.E.M. (n=6).

CONCLUSION

Based on the results of this study, we conclude that NP-L33s has a lower propensity than NP-L20 to induce the ABC phenomenon and a good sustained-release profile of PGE_1, which may be clinically useful.

ACKNOWLEDGEMENTS

This work was supported by Grants-in-Aid for Scientific Research from the Ministry of Health, Labour, and Welfare of Japan, as well as the Japan Science and Technology Agency and Grants-in-Aid for Scientific Research from the Ministry of Education, Culture, Sports, Science and Technology, Japan.

REFERENCES

1. Maeda H, Wu J, Sawa T, Matsumura Y, Hori K. Tumor vascular permeability and the EPR effect in macromolecular therapeutics: a review. J Control Release. 2000;65:271–84.
2. Gref R, Minamitake Y, Peracchia MT, Trubetskoy V, Torchilin V, Langer R. Biodegradable long-circulating polymeric nanospheres. Science 1994;263:1600–3.
3. Stolnik S, Dunn SE, Garnett MC, Davies MC, Coombes AG, Taylor DC, *et al.* Surface modification of poly(lactide-co-glycolide) nanospheres by biodegradable poly(lactide)-poly(ethylene glycol) copolymers. Pharm Res. 1994;11:1800–8.
4. Ishihara T, Takahashi M, Higaki M, Takenaga M, Mizushima T, Mizushima Y. Prolonging the *in vivo* residence time of prostaglandin E(1) with biodegradable nanoparticles. Pharm Res. 2008;25:1686–95.
5. Sharpe M, Easthope SE, Keating GM, Lamb HM. Polyethylene glycol-liposomal doxorubicin: a review of its use in the management of solid and haematological malignancies and AIDS-related Kaposi's sarcoma. Drugs 2002;62:2089–126.
6. Dams ET, Laverman P, Oyen WJ, Storm G, Scherphof GL, van Der Meer JW, *et al.* Accelerated blood clearance and altered biodistribution of repeated injections of sterically stabilized liposomes. J Pharmacol Exp Ther. 2000;292:1071–9.
7. Ishida T, Maeda R, Ichihara M, Mukai Y, Motoki Y, Manabe Y, *et al.* The accelerated clearance on repeated injection of pegylated liposomes in rats: laboratory and histopathological study. Cell Mol Biol Lett. 2002;7:286.
8. Ishida T, Kiwada H. Accelerated blood clearance (ABC) phenomenon upon repeated injection of PEGylated liposomes. Int J Pharm. 2008;354:56–62.
9. Wang XY, Ishida T, Ichihara M, Kiwada H. Influence of the physicochemical properties of liposomes on the accelerated blood clearance phenomenon in rats. J Control Release. 2005;104:91–102.
10. Laverman P, Carstens MG, Boerman OC, Dams ET, Oyen WJ, van Rooijen N, *et al.* Factors affecting the accelerated blood clearance of polyethylene glycol-liposomes upon repeated injection. J Pharmacol Exp Ther. 2001;298:607–12.
11. Ishida T, Ichihara M, Wang X, Yamamoto K, Kimura J, Majima E, *et al.* Injection of PEGylated liposomes in rats elicits PEG-specific IgM, which is responsible for rapid elimination of a second dose of PEGylated liposomes. J Control Release. 2006;112:15–25.
12. Ishida T, Atobe K, Wang X, Kiwada H. Accelerated blood clearance of PEGylated liposomes upon repeated injections: effect of doxorubicin-encapsulation and high-dose first injection. J Control Release. 2006;115:251–8.
13. Ishida T, Masuda K, Ichikawa T, Ichihara M, Irimura K, Kiwada H. Accelerated clearance of a second injection of PEGylated liposomes in mice. Int J Pharm. 2003;255:167–74.
14. Ishida T, Maeda R, Ichihara M, Irimura K, Kiwada H. Accelerated clearance of PEGylated liposomes in rats after repeated injections. J Control Release. 2003;88:35–42.
15. Wang X, Ishida T, Kiwada H. Anti-PEG IgM elicited by injection of liposomes is involved in the enhanced blood clearance of a subsequent dose of PEGylated liposomes. J Control Release. 2007;119:236–44.
16. Ishida T, Ichihara M, Wang X, Kiwada H. Spleen plays an important role in the induction of accelerated blood clearance of PEGylated liposomes. J Control Release. 2006;115:243–50.
17. Ishida T, Wang X, Shimizu T, Nawata K, Kiwada H. PEGylated liposomes elicit an anti-PEG IgM response in a T cell-independent manner. J Control Release. 2007;122:349–55.
18. Ishida T, Kashima S, Kiwada H. The contribution of phagocytic activity of liver macrophages to the accelerated blood clearance (ABC) phenomenon of PEGylated liposomes in rats. J Control Release. 2008;126:162–5.
19. Caro J, Migliaccio-Walle K, Ishak KJ, Proskorovsky I. The morbidity and mortality following a diagnosis of peripheral arterial disease: long-term follow-up of a large database. BMC Cardiovasc Disord. 2005;5:14.
20. Chandra Sekhar N. Effect of eight prostaglandins on platelet aggregation. J Med Chem. 1970;13:39–44.
21. Simmet T, Peskar BA. Prostaglandin E1 and arterial occlusive disease: pharmacological considerations. Eur J Clin Invest. 1988;18:549–54.
22. Carlson LA, Olsson AG. Intravenous prostaglandin E1 in severe peripheral vascular disease. Lancet. 1976;2:810.
23. Belch JJ, Bell PR, Creissen D, Dormandy JA, Kester RC, McCollum RD, *et al.* Randomized, double-blind, placebo-controlled study evaluating the efficacy and safety of AS-013, a prostaglandin E1 prodrug, in patients with intermittent claudication. Circulation 1997;95:2298–302.
24. Ferreira SH, Vane JR. Prostaglandins: their disappearance from and release into the circulation. Nature 1967;216:868–73.
25. Golub M, Zia P, Matsuno M, Horton R. Metabolism of prostaglandins A1 and E1 in man. J Clin Invest. 1975;56:1404–10.
26. Monkhouse DC, Van Campen L, Aguiar AJ. Kinetics of dehydration and isomerization of prostaglandins E 1 and E 2. J Pharm Sci. 1973;62:576–80.
27. Mizushima Y, Yanagawa A, Hoshi K. Prostaglandin E1 is more effective, when incorporated in lipid microspheres, for treatment of peripheral vascular diseases in man. J Pharm Pharmacol. 1983;35:666–7.
28. Mizushima Y. Lipo-prostaglandin preparations. Prostaglandins Leukot Essent Fatty Acids. 1991;42:1–6.
29. Mizushima Y. Lipid microspheres as novel drug carriers. Drugs Exp Clin Res. 1985;11:595–600.
30. Mizushima Y, Hamano T, Haramoto S, Kiyokawa S, Yanagawa A, Nakura K, *et al.* Distribution of lipid microspheres incorporating prostaglandin E1 to vascular lesions. Prostaglandins Leukot Essent Fatty Acids. 1990;41:269–72.
31. Igarashi R, Mizushima Y, Takenaga M, Matsumoto K, Morizawa Y, Yasuda A. A stable PGE1 prodrug for targeting therapy. J Control Release. 1992;20:37–46.
32. Yoshida T, Uetake A, Yamaguchi H, Nimura N, Kinoshita T. New preparation method for 9-anthryldiazomethane (ADAM) as a fluorescent labeling reagent for fatty acids and derivatives. Anal Biochem. 1988;173:70–4.
33. Ishihara T, Takahashi M, Higaki M, Mizushima Y. Efficient encapsulation of a water-soluble corticosteroid in biodegradable nanoparticles. Int J Pharm. 2009;365:200–5.
34. Ishihara T, Izumo N, Higaki M, Shimada E, Hagi T, Mine L, *et al.* Role of zinc in formulation of PLGA/PLA nanoparticles encapsulating betamethasone phosphate and its release profile. J Control Release. 2005;105:68–76.
35. Bazile D, Prud'homme C, Bassoullet MT, Marlard M, Spenlehauer G, Veillard M. Stealth Me.PEG-PLA nanoparticles avoid uptake by the mononuclear phagocytes system. J Pharm Sci. 1995; 84:493–8.
36. Ishida T, Harada M, Wang XY, Ichihara M, Irimura K, Kiwada H. Accelerated blood clearance of PEGylated liposomes following preceding liposome injection: effects of lipid dose and PEG surface-density and chain length of the first-dose liposomes. J Control Release. 2005;105:305–17.
37. Lee SW, Chang DH, Shim MS, Kim BO, Kim SO, Seo MH. Ionically fixed polymeric nanoparticles as a novel drug carrier. Pharm Res. 2007;24:1508–16.

38. Musumeci T, Ventura CA, Giannone I, Ruozi B, Montenegro L, Pignatello R, *et al.* PLA/PLGA nanoparticles for sustained release of docetaxel. Int J Pharm. 2006;325:172–9.
39. Koide H, Asai T, Hatanaka K, Urakami T, Ishii T, Kenjo E, *et al.* Particle size-dependent triggering of accelerated blood clearance phenomenon. Int J Pharm. 2008;362:197–200.
40. Lu W, Wan J, She Z, Jiang X. Brain delivery property and accelerated blood clearance of cationic albumin conjugated pegylated nanoparticle. J Control Release. 2007;118:38–53.
41. Richter AW, Akerblom E. Polyethylene glycol reactive antibodies in man: titer distribution in allergic patients treated with monomethoxy polyethylene glycol modified allergens or placebo, and in healthy blood donors. Int Arch Allergy Appl Immunol. 1984;74:36–9.

Protective role of HSF1 and HSP70 against gastrointestinal diseases

Ken-ichiro Tanaka and Tohru Mizushima

Graduate School of Medical and Pharmaceutical Sciences, Kumamoto University, Kumamoto 862-0973, Japan

Running title: HSP70 and gastrointestinal diseases

Address correspondence to: Dr. Tohru Mizushima, Graduate School of Medical and Pharmaceutical Sciences, Kumamoto University, 5-1 Oe-honmachi, Kumamoto 862-0973, Japan. TEL & FAX: 81-96-371-4323 E-mail: mizu@gpo.kumamoto-u.ac.jp

ABSTRACT

Purpose: It is well known that heat shock proteins (HSPs) are induced by various stressors in order to confer protection against such stressors. Since stressor-induced tissue damage is involved in various diseases, especially gastrointestinal diseases, it has been thought that HSP-inducers are therapeutically beneficial for these diseases. Indirect lines of evidence suggest that HSPs provide a major protective mechanism against irritant-induced gastric lesions. However, no direct evidences that support this notion exits. On the other hand, inflammatory bowel disease (IBD) involves infiltration of leukocytes into intestinal tissue, resulting in intestinal damage. Pro-inflammatory cytokines and cell adhesion molecules (CAMs) play important roles in this infiltration of leukocytes. The roles of heat shock factor 1 (HSF1, a transcription factor for *hsp* genes) and heat shock proteins (HSPs) in development of IBD are unclear. In this paper, we reviewed our recent work on the role of HSPs in pathogenesis of gastric lesions and IBD by use of HSF1-null mice and transgenic mice expressing HSP70. **Conclusion.** This study provides the first genetic evidence that HSF1 and HSP70 play a role in protecting against both irritant-induced gastric lesions and IBD-related colitis. The

aggravation of irritant-induced gastric lesions in HSF1-null mice is due to their inability to up-regulate HSP70, leading to apoptosis. On the other hand, this protective role of HSP70 against colitis seems to involve various mechanisms, such as suppression of expression of pro-inflammatory cytokines and CAMs, and cell death.

INTRODUCTION

The balance between aggressive and defensive factors determines development of gastric lesions. The gastric mucosa is challenged by a variety of both endogenous and exogenous irritants (aggressive factors), including ethanol, gastric acid, pepsin, non-steroidal anti-inflammatory drugs (NSAIDs) and *Helicobacter pylori*. These irritants damage the mucosal cells, inducing cell death which leads to the formation of gastric lesions [1]. In order to protect the gastric mucosa, a complex defence system, which includes the production of surface mucus and bicarbonate and the regulation of gastric mucosal blood flow (GMBF), has evolved. Prostaglandins (PGs), in particular PGE_2, enhance these protective mechanisms, and are therefore thought to comprise a major gastric mucosal defensive factor [2].

Recently, heat shock proteins (HSPs) have also attracted considerable attention as another major defensive factor. When cells are exposed to stressors, a number of so-called stress proteins are induced, in order to confer protection against such stressors. HSPs are representative of these stress proteins, and their cellular up-regulation, especially that of HSP70, provides resistance as they re-fold or degrade denatured proteins produced by the stressors [3]. It has been reported not only that various gastric irritants, including ethanol, up-regulate HSPs, but also that artificial up-regulation of HSPs confers resistance to these irritants in cultured gastric mucosal cells [3]. Although these findings strongly indicate that HSPs are protective, very little direct evidence exists, and to date no *in vivo* study has been conducted to demonstrate that inhibition of HSPs results in a phenotype susceptible to irritant-induced gastric lesions.

Interestingly, geranylgeranylacetone (GGA), a leading anti-ulcer drug on the Japanese market, has been reported to be a non-toxic HSP-inducer, up-regulating various HSPs not only in cultured gastric mucosal cells at concentrations that do not affect cell viability but also in various tissues, including the gastric mucosa *in vivo* [4, 5]. We have previously reported that pre-induction of HSPs by GGA protects cultured

gastric mucosal cells from cell death induced by various irritants [6-9]. These previous results suggest that the anti-ulcer effect of GGA is due to its HSP-inducing activity. However, because GGA mediates various other gastro-protective mechanisms [10, 11], it remains unclear whether up-regulation of HSPs represents GGA's major mode of anti-ulcer activity. The up-regulation of HSPs by various stressors is regulated at the transcription level by a consensus *cis*-element (heat shock element (HSE)) and a transcription factor (heat shock factor 1 (HSF1)), that specifically binds to HSE located on the upstream region of *hsp* genes [12].

Inflammatory bowel disease (IBD), Crohn's disease (CD) and ulcerative colitis (UC), have become substantial health problems with an actual prevalence of 200-500 per 100,-000 people in western countries, which almost doubles every 10 years [13]. Although the etiology of IBD is not yet fully understood, recent studies suggest that IBD involves chronic inflammatory disorders in the intestine due to "a vicious cycle". Infiltration into intestinal tissues cause intestinal mucosal damage induced by reactive oxygen species (ROS) that are released from the activated leukocytes, and this intestinal mucosal damage further stimulates the infiltration of leukocytes [14]. To understand

the molecular mechanism underlying the pathogenesis of IBD and to develop new types of clinical drugs for IBD, identification of endogenous factors that positively or negatively affect the development of IBD is important. For this purpose, various experimental animal colitis models, in particular the dextran sulfate sodium (DSS)-induced colitis models, have been used [15]. Pro-inflammatory cytokines and cell adhesion molecules (CAMs) play an important role in the activation and infiltration of leukocytes that is associated with IBD [16, 17].

HSPs and HSF1 also have attracted considerable attention as candidates for endogenous factors that affect the development of IBD because some HSPs, including HSP70, were reported to be over-expressed in the intestinal tissues of IBD patients and in an animal model of IBD [18]. HSF1 negatively regulates the expression of *tnf*-α and *il-1*β genes [19]. These previous results suggest that HSPs and HSF1 have negative roles on the development of IBD, however, there is no direct evidence (such as genetic evidence) to support this idea. Furthermore, there are some data that suggest positive roles for HSPs and HSF1 in the development of IBD [20]. Therefore, the effects of genetic alteration of HSPs and HSF1 on the development of colitis in animal models of

IBD should be examined in order to understand the exact role (positive or negative) of HSPs and HSF1 in IBD.

In this review, we summarized our recent work using HSF1-null mice and transgenic mice expressing HSP70 to obtain direct genetic evidence for the contribution of HSPs to the protection of the gastric mucosa and to examine the role of HSF1 and HSPs in the pathogenesis of DSS-induced colitis.

RESULTS

The Role of HSF1 and HSPs in Gastric Ulcerogenic Response. We examined the role of HSF1 in gastric ulcerogenic response by use of HSF1-null mice [21]. As shown in Fig. 1A, intragastric administration of 40% ethanol resulted in significant gastric lesions in HSF1-null mice but not in wild-type mice. These results show that HSF1 plays an important role in protecting the gastric mucosa from ethanol-induced lesions. Similar results were obtained with hydrochloric acid-induced gastric lesions (Fig. 1B). Given that HSF1 up-regulates the expression of HSPs, we examined the effect of

ethanol administration on the expression of HSPs in the gastric mucosa of HSF1-null mice and wild-type mice. Ethanol administration up-regulated the production of only HSP70, a response that was dependent on the function of HSF1 (Fig. 1C). Based on these results, we subsequently focused on HSP70.

In order to investigate the mechanism governing the severity of production of ethanol-stimulated gastric lesions in HSF1-null mice, we compared the level of apoptosis. In wild-type mice, an increase in TUNEL-positive (apoptotic) cells was observed following the administration of 100% but not 40% ethanol, whereas a clear increase in TUNEL-positive cells was observed with 40% ethanol administration in the HSF1-null mice [21]. These results show that induction of apoptosis by ethanol is enhanced in HSF1-null mice compared to wild-type mice; in other words, HSF1 protects gastric mucosal cells from ethanol-induced apoptosis.

Another group also suggested the protective role of HSPs (HSP27) against irritant-induced gastric lesions. HSP27 also has cytoprotective effect. Ebert *et al.* reported that transgenic mice expressing HSP27 showed resistant phenotype to indometacin-induced gastric lesions. They also showed that overexpression of HSP27